

Enhanced Sensitivity of Electrochemical Biosensor on Microfluidic Paper Based Analytical Device Using ZnO/MWCNTs Nanocomposite

Roekmono¹, Harsono Hadi¹, Hilya Nur Imtihani², Luthviah Choiratul Muhimmah¹, Rio Akbar Yuwono³, Ruri Agung Wahyuono^{1*}

¹Department of Engineering Physics, Institut Teknologi Sepuluh Nopember, Surabaya, 60111, Indonesia

²Surabaya Pharmacy Academy, Surabaya, 60232, Indonesia

³Graduate Institute of Applied Science and Technology, National Taiwan University of Science and Technology, Taipei, 10607, Taiwan

Received: 4th Dec, 18; Revised: 19th Feb, 19, Accepted: 14th Mar, 19; Available Online: 25th Jun, 2019

ABSTRACT

This paper presents an integrated ZnO/multi-walled carbon nanotubes (MWCNTs) electrode in novel stacking paper-based microfluidic analytical device for electrochemical biosensor. The designed sensors were subjected to detect glucose and ascorbic acid in a simulated body fluid using electrochemical methods, including cyclic voltammetry and impedance spectroscopy. The composite of ZnO/multi-walled carbon nanotubes (MWCNTs) with variations in mass fractions of 0.1, 0.5, 1, 2, 4 and 8% MWCNTs for measuring ascorbic acid and glucose with concentrations spanning from 0.02 to 5.12 mM. The best results are obtained by 2% of MWCNTs in composited electrode, in which linear characteristics ($R^2 > 0.8$) of the current response value show a sensitivity (gradient) of 0.017 and 0.085 $\mu\text{A}/\text{mM}\cdot\text{cm}^2$ for ascorbic acid and glucose measurement, respectively. The electrochemical detection by means of impedance spectra shows a linearly decreasing trend of chemical capacitance with increasing concentration of glucose and ascorbic acid. However, in the present system it is not sufficient to specifically distinguish the frequency response associated to glucose and ascorbic acid.

Keywords: Glucose; Ascorbic Acid; ZnO; MWCNTs; Cyclic Voltammetry, Impedance Spectroscopy.

INTRODUCTION

The conventional clinical diagnosis devices are one of the intriguing challenges to the future health system: The prices are relatively expensive and the devices require a long time to diagnose and special expertise in operations^{1,2}. The development of the affordable and portable diagnostic devices recently becomes one of the central issue in the health system¹⁻³. In particular, the use of microfluidic devices for blood plasma separation methods is considered to replace conventional clinical diagnosis devices^{1,3}. The World Health Organization (WHO) has provided criteria for portable clinical diagnosis tools: *affordable, sensitive, specific user-friendly, rapid and robust, equipment free, deliverable to end users*⁴.

Paper-based microfluidic devices (microfluidic paper-based analytical devices, μPADs) are the emerging platform for blood plasma separation as well as considered to meet the abovementioned criteria for clinical diagnosis devices⁵⁻⁷. In addition, μPADs are a green technology which are easy to dispose and to decompose. In principle, μPADs exploit the virtue by capillary effect of fluid flow in paper as porous medium so that there is no need for external forces to drive the fluid flow^{8,9}. Currently, there exist several detection methods for measuring targeted bio-substances for clinical diagnosis in μPADs , *i.e.*, electrochemiluminescence, colorimetry, fluorescence, and electrochemical. Of the various methods that have been

developed, electrochemical detection is by far the most used method for biosensing in μPADs ¹⁰⁻¹³.

The electrochemical detection method by means of cyclic voltammetry (CV) in μPADs has successfully been performed to be able to detect glucose level with distinctive sensitivity¹⁴. Other electrochemical method, *i.e.*, electrochemical impedance spectroscopy (EIS), in μPADs to detect glucose levels has been carried out as well¹⁴. Both studies succeeded in detecting glucose levels by integrating μPADs with ZnO nanoparticles so as to produce a high sensitivity detection. Nonetheless, these μPADs didn't use blood as the main fluid, so that the results couldn't show the separation of blood plasma perfectly. Recent researches reported the improved the design of μPADs by using two stacking layers of filter paper decorated with ZnO nanoflowers and ZnO spherical aggregates which can separate plasma from blood samples and is used to detect glucose spectroscopically^{15,16}.

In this study, the optimized microfluidic design^{15,16} will be further utilized as an active electrode for electrochemical biosensor. The surface of ZnO nanoparticles will be composited with multiwalled-carbon nanotubes (MWCNTs) with the aim at increasing the sensitivity of electrochemical detection due to the high conductivity of MWCNTs. The microfluidic paper-based biosensors will be assessed to detect ascorbic acid and glucose content in the simulated body fluid. Thus, the developed paper-based

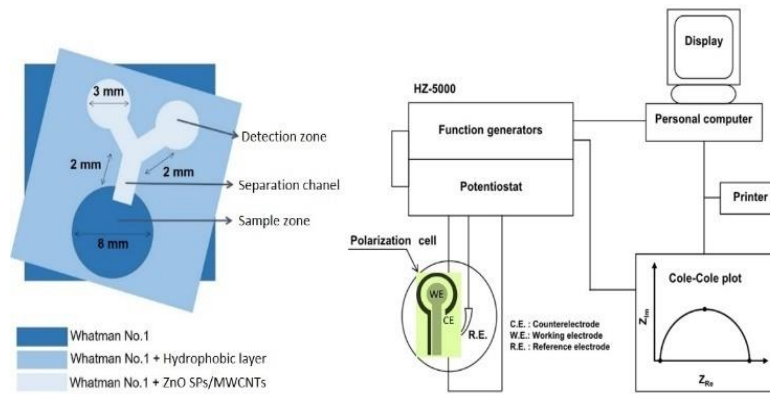


Figure 1: Design and geometry of ZnO/MWCNTs (WE) electrode on paper-based microfluidic designed by Muhimmah et al (2018). Carbon circuit was printed around the detection zone and separation channel.

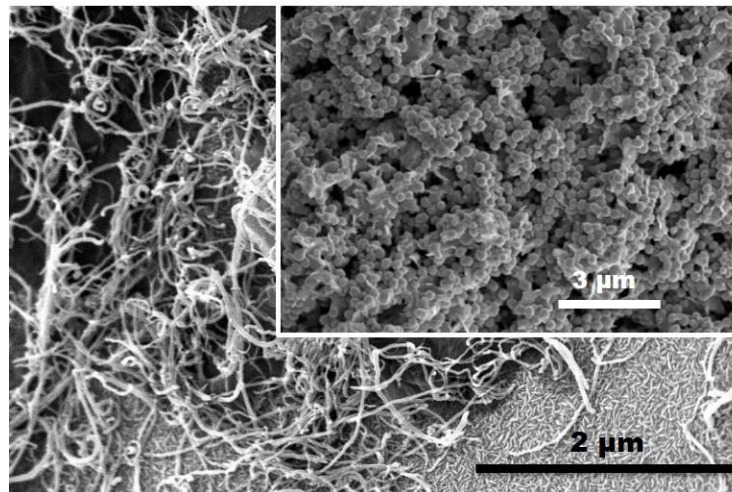


Figure 2: Scanning electron microscopic image of MWCNTs and ZnO/MWCNTs nanocomposite with 0.1% mass of MWCNTs (inset).

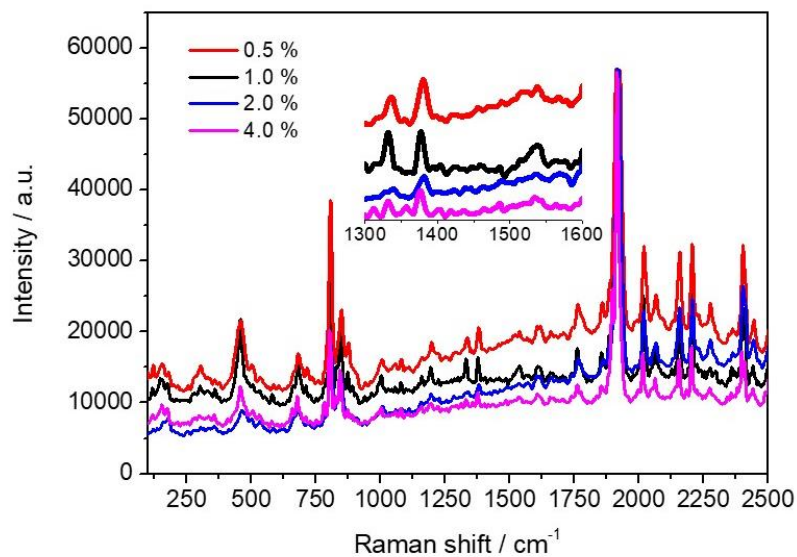


Figure 3: Selected Raman spectra of ZnO/MWCNTs nanocomposites.

microfluidic biosensors are not only able to separate blood plasma but can also be used to detect bio-target compounds using electrochemical methods.

MATERIALS AND METHOD

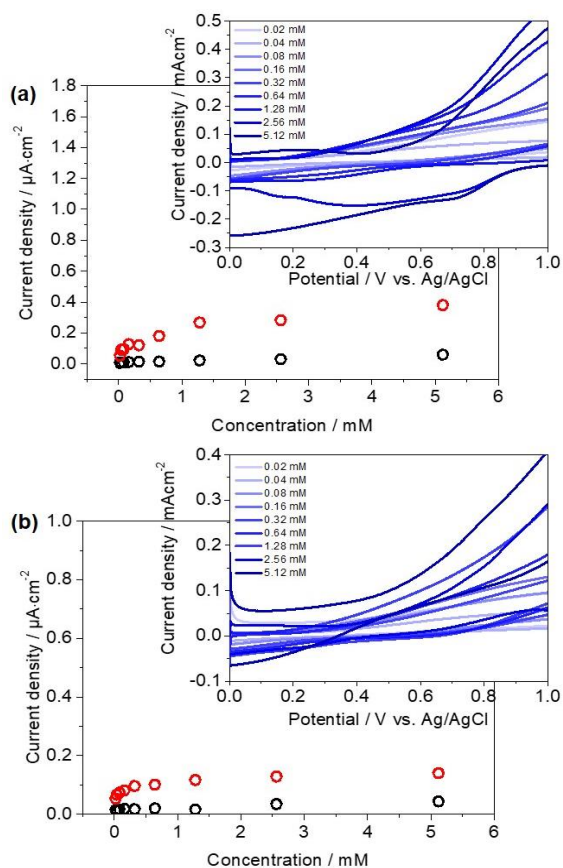


Figure 4: CV output current response for nanocomposite use with variations in mass fractions MWCNTs 0.1 (a) and 2% (b). Dark circles for response to ascorbic acid, red circles for glucose response.

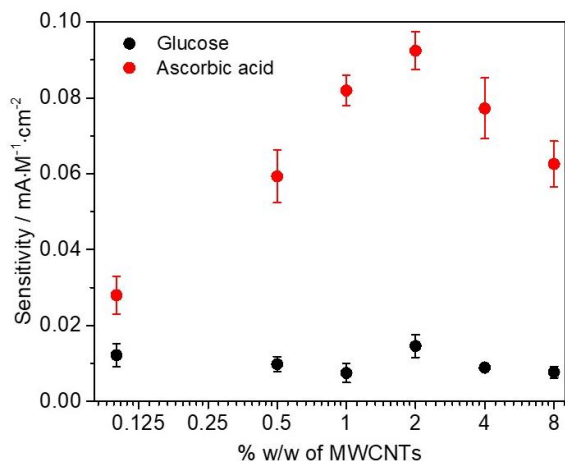


Figure 5: Sensitivity of glucose and ascorbic acid measurements from the current density response of cyclic voltammogram. The error bar is calculated from three individual measurements.

Preparation and Characterization of ZnO/MWCNTs Composite

ZnO nanoparticles were synthesized by the wet chemical method^{17,18}. An 0.1 M of Zn(CH₃COOH)₂·2H₂O in diethylene glycol solvent was stirred and heated at a temperature of 200°C for 2 hours until the solution turned

into milky-white. The ZnO nanoparticles were obtained by centrifugation of the resultant solution to separate ZnO nanoparticles with the solvent and the remaining reaction products. To form ZnO/MWCNTs nanocomposites through covalent bonds, MWCNTs (Cheaptubes Inc) were oxidized with nitric acid in reflux at 130°C for 10 hours. Subsequently, the MWCNTs solution is diluted with water and filtered. MWCNTs which are functionalized by COOH groups are obtained after several washings with water and dried at 75°C for 12 hours.

Nano ZnO Particles Characterization

ZnO micro morphology was analyzed from the Scanning Electron Microscopy (SEM) FEI Inspect-S50 test which operated at a 20.0 kV voltage acceleration. The pore characteristics and active surface area of ZnO were tested using the Brunauer, Emmett, Teller (BET) method in a nitrogen atmosphere at 77 K as reported by ref.^{19,20}.

Sensor Fabrication on Paper-Based Microfluidic

Paper-based microfluidics decorated with ZnO nanoparticles are designed as in Fig. 1. The microfluidic design was adopted from geometry designed in our previous work¹⁵. The separation channel to the detection zone is coated with ZnO/MWCNTs composites and becomes a working electrode of electrochemical sensor. The counter electrode was prepared using a conductive carbon paste (Solaronix) that is printed using a mask in the area around the separation channel and detection zone to form carbon circuits.

Glucose and Ascorbic Acid Sensing

Simulated body fluid (SBF) was used as the supporting electrolytes for glucose and ascorbic acid to replace body fluids, which is blood serum. The protocol to prepare SBF was described elsewhere²¹. The SBF contained KCl, K₂HPO₄·3H₂O, MgCl₂·6H₂O, CaCl₂, and Na₂SO₄. The concentrations of glucose and ascorbic acid investigated in this study were 0.02, 0.04, 0.08, 0.16, 0.32, 0.64, 1.28, 2.56, and 5.12 mM. For electrochemical measurements, cyclic voltammetry and electrochemical impedance spectroscopy were employed. The counter electrode was a carbon electrode printed on the μ -PAD, and the reference to oxidation potential was Ag/AgCl wire. The current-voltage response of the cyclic voltammetry measurement and the impedance spectroscopy were carried out using Versastat II potentiostat/galvanostat aided with frequency response analyzer.

RESULTS AND DISCUSSIONS

The surface morphology of paper electrodes that have been coated with nano ZnO/MWCNTs composite is depicted in Figure 2. MWCNTs utilized here has tube diameter spanning from 30 – 50 nm with average length of 10 – 20 μ m. Upon compositing MWCNTs to ZnO, it is shown that ZnO nanoparticles are decorated with MWCNTs and agglomerated due to the very long MWCNTs over the size of ZnO aggregates. The individual morphology of ZnO nanoparticles is in the form of spherical aggregates with sizes varying from 200 to 300 nm. As the ZnO spherical aggregates have been intensively investigated in our group^{16,19}, this spherical aggregate is composed of primary crystallites of 15-20 nm and exhibits an active surface area

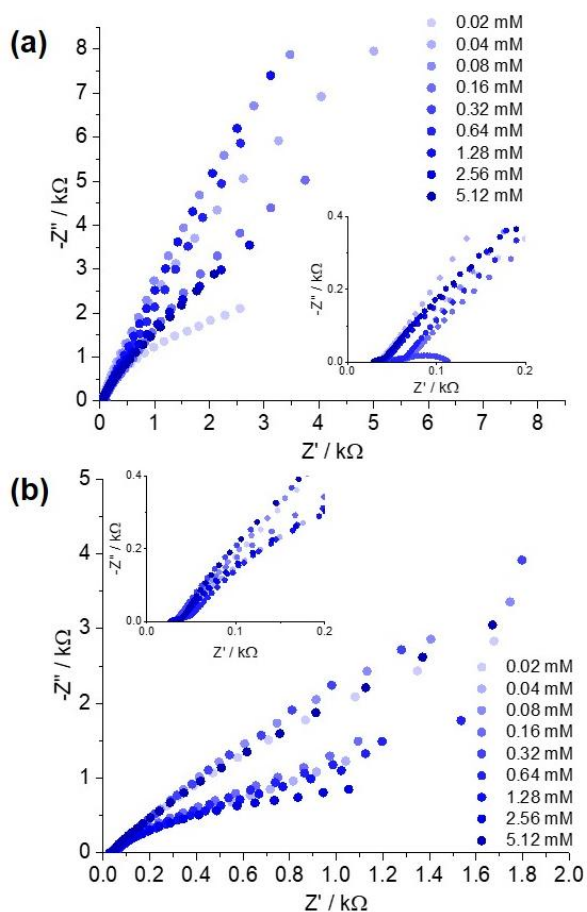


Figure 6: Nyquist plot of for nanocomposite use with variations in mass fractions MWCNTs of 0.1 (a) and 2% (b).

of 30-100 m^2/g . The primary ZnO crystallites in outer spherical geometry provide active area for MWCNTs functionalization *via* -COOH covalent bond. A qualitative view of composite formation from SEM images (inset of Fig. 2) indicates that the covalent bond of -COOH in MWCNTs to the surface of ZnO is not homogeneous. This nonhomogeneous functionalization is very reasonable for preparation of nanocomposites through wet chemical synthesis.

To assign the electronic properties of different ZnO/MWCNTs nanocomposites, Raman spectra are recorded. Raman spectra of ZnO/MWCNTs nanocomposites are depicted in Fig. 3 for different mass fraction of MWCNTs. The identification of ZnO nanoparticles can be seen in the wavenumber (Raman shift) below 800 cm^{-1} . Raman peak at 450 cm^{-1} is a typical second order Raman mode for ZnO nanoparticles with a Wurtzite hexagonal crystal structure²². Raman peaks at 500 and 700 cm^{-1} indicate the spectral identifier of the optical phonon mode of ZnO surface. Identification of MWCNTs on the electrodes can be observed from the Raman spectrum at wavenumbers (Raman shift) of 1315 and 1585 cm^{-1} ²³. The Raman scattering peak at 1315 cm^{-1} is a spectral identifier of the D band (disorder) derived from amorphous carbon and defects in the structure of carbon atoms. Meanwhile, the Raman peaks at 1585 cm^{-1} (G band, graphite) are associated with shear modes of carbon atoms,

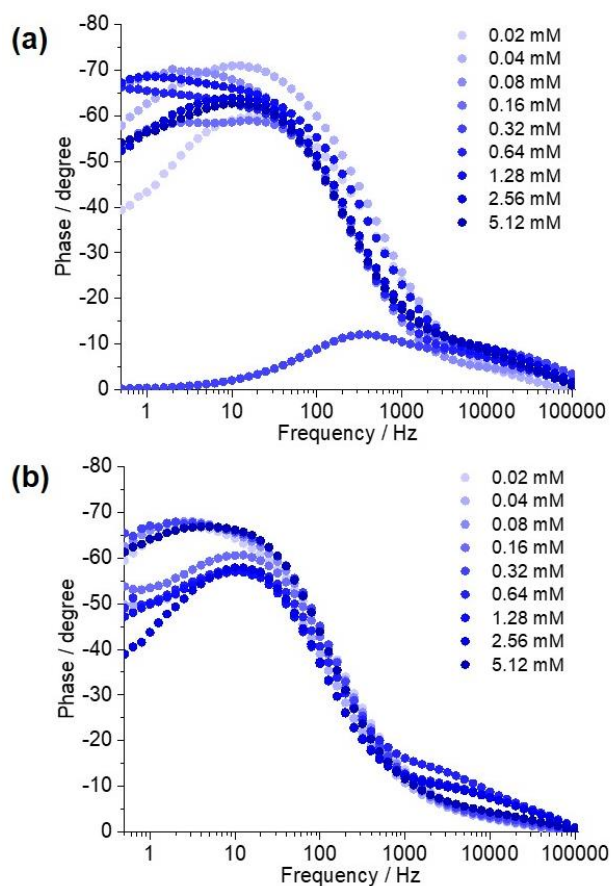


Figure 7: Bode plot of for nanocomposite use with variations in mass fractions MWCNTs of 0.1 (a) and 2% (b).

and the peak of Raman at 2650 cm^{-1} is the overtone of the D band. The other Raman peaks can be attributed to the Raman scattering effect of the paper substrate. In general, the addition of mass fractions of MWCNTs does not affect the electronic character of ZnO nanoparticle because there is no shift in the Raman scattering peak. However, the defect of the carbon atom structure in MWCNTs is slightly altered as the intensity ratio of the D band to G band ($I_{D/G}$) is modified (see inset of Fig. 3). This $I_{D/G}$ gives an estimated concentration of defects in MWCNTs. As shown, the $I_{D/G}$ tends to decrease with increasing concentration of MWCNTs up to 2%. The $I_{D/G}$ increases again for 4% and 8% mass fraction of MWCNTs. This result indicates that 2% MWCNTs in nanocomposites provide minimum defects on MWCNTs.

Electrochemical measurements by using cyclic voltammetry (CV) was carried out to obtain the specific current response toward different concentration of glucose and ascorbic acid. The cyclic voltamogram on the simulated body fluid containing various concentrations of glucose and ascorbic acid are shown in Fig. 4. In general, the use of a MWCNTs in nanocomposites has improved electrochemical current density response within voltage range $0-2\text{ V}$ (vs. Ag/AgCl). As can be seen, some oxidation peaks, albeit less prominent, at voltages of $\pm 0.2\text{ V}$, $\pm 0.5\text{ V}$, $\pm 1.3\text{ V}$, and $\pm 1.7\text{ V}$ can be readily observed on the curve.

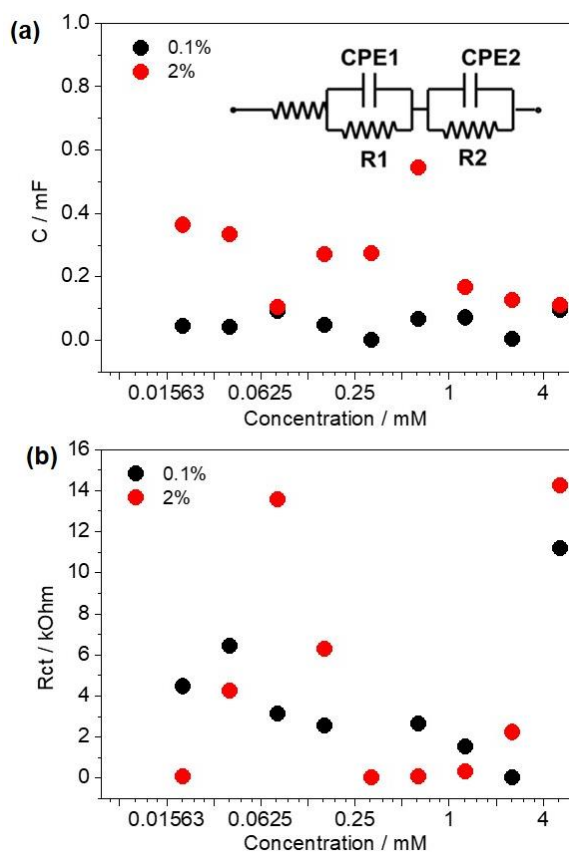


Figure 8: (a) Chemical capacitance and (b) The charge transfer resistance at the interface of electrode and SBF containing glucose and ascorbic acid. Inset shows the equivalent circuit model to extract the electric properties from impedance data.

To assign the oxidation potential toward target compound, we have measured the oxidation potential of glucose and ascorbic acid individually (data not shown) using glassy carbon electrode. The oxidation potential of glucose and ascorbic acid is 0.22 and 0.37 V, respectively. These results are in good agreement with literatures^{24,25}, in which the oxidation potential of ascorbic acid and glucose with reference voltage Ag/AgCl are 0.28 V and 0.4 V, respectively. Therefore, the peak potentials at ± 0.2 V and ± 0.5 V are considered as the target analysis. On the other hand, oxidation peaks (local maximum curve) > 1 V is neglected which are possibly due to the oxidation of other bio-materials from paper material and other components in the SBF.

Quantitative analysis of CV current response to emphasize the electrode sensitivity is shown in Fig. 5. In general, 2% mass fraction of MWCNTs in ZnO/MWCNTs nanocomposites exhibit the best sensitivity of all other nanocomposites. For 0.1% mass fraction of MWCNTs, linear response ($R^2 > 0.8$) was only obtained for ascorbic acid and glucose concentrations up to 1.28 mM. The sensitivity of the current response for ascorbic acid is $0.051 \mu\text{A}/\text{mM}\cdot\text{cm}^2$ and the sensitivity of glucose is $0.061 \mu\text{A}/\text{mM}\cdot\text{cm}^2$, with an integral current response of 6 - 9% of the total recorded CV current response. For 2% and 8% mass fractions of MWCNTs, a linear response was

obtained for the concentration of ascorbic acid and glucose up to 5.12 mM. The integration of current responses of glucose and ascorbic acid for 2 and 8% fractions of MWCNTs from the total CV currents are 10-35% and 16-40%, respectively. The sensitivity of ascorbic acid measurement was 0.015 and $0.009 \mu\text{A}/\text{mM}\cdot\text{cm}^2$ for mass fractions of 2 and 8%, while the sensitivity of glucose measurement was 0.082 and $0.077 \mu\text{A}/\text{mM}\cdot\text{cm}^2$ for mass fractions 2 and 8%.

The above results indicate that 0.1% mass of MWCNTs is not able to widen the sensor range for large concentrations. The reduced sensitivity of measurements for larger MWCNTs concentration (4 and 8%) can be due to the reduced total reactivity and the increasing number of defects in MWCNTs as revealed from Raman spectra. In addition, ZnO is a nanoparticle with rich surface defects that are intentionally used for sensor applications. Likewise, for MWCNTs the bent surface has a high reactivity where the number of nanotubes grooves will decrease if MWCNTs are homogeneously aligned due to the assembly process when composting. At high concentrations, the closed chemical surface of ZnO by MWCNTs which is also reactive to the bio compounds reduces the total reactivity to sense and measure bio compounds, so that the sensitivity of electrode decreases.

Having laid the analysis of electrochemical detection by means of cyclic voltammetry, the results of electrochemical detection of glucose and ascorbic acid in simulated body fluids by means of impedance spectroscopy are now discussed and depicted in Fig. 6 and Fig. 7. The Nyquist plot shows two semicircle in the high frequency and medium frequency regime. The small semicircle in frequency range of 10 - 100 kHz is attributed to the charge transfer at carbon counter electrodes. The big semicircle in frequency range of 1 - 10 kHz indicates the charge transfer at the interface of ZnO/MWCNTs/SBF containing glucose and ascorbic acid. It is clear that the impedance response of 0.1% MWCNTs in nanocomposite electrode has bigger value than that of 2% MWCNTs. Irrespective of mass fraction of MWCNTs on nanocomposites, the impedance response, both the real impedance (Z' , resistance) and the imaginary impedance (Z'' , capacitance) tends to decrease with increasing concentration of bio-compound. The Bode plot (see Fig. 7) indicates a non-systematic shift of frequency peaks with increasing concentration of glucose and ascorbic acid. This shift shows the different lifetimes of charge accumulated in the electrode, that is shifting to lower frequency indicating a longer lifetime. Nonetheless, the frequency response is broadened in low frequency regime and hence, it is difficult to distinguish the peak frequency of glucose and ascorbic acid since the difference frequency response of both target compound is insignificant.

To extract meaningful properties from impedance spectra, a quantitative analysis is carried out by fitting the impedance data with equivalent circuit model, *i.e.*, two serial of modified Randle circuit with additional sheet resistance (see inset of Fig. 8a)²⁶. Since the capacitive effect doesn't behave ideally, a constant phase element (CPE) - pseudo capacitor - substitutes the role of

capacitor. The pseudo capacitor will give a pseudo capacitance (Q) and non-ideality factor (α). The chemical capacitance is then calculated by the following formula: $C = R^{(1-\alpha)/\alpha} \times Q^{1/\alpha}$. The fitting results, particularly the capacitance (C) and charge transfer resistance (R_{ct}) at the interface of ZnO/MWCNTs/SBF, for 0.1% and 2% MWCNTs concentration are depicted in Fig. 8. As also qualitatively discussed earlier, the charge transfer resistance and capacitance are likely linearly decreasing with the increasing concentration of glucose and ascorbic acid. While the R_{ct} value does not differ significantly between 0.1% and 2% MWCNTs concentration, the capacitance of 2% MWCNTs is marked higher than that of 1% MWCNTs and other concentration (data not shown). Although the capacitance measurements derived from impedance show linear model, the shortcoming of the present system is rooted from the ability to distinguish responses from different bio components.

CONCLUSION

The paper-based electrochemical biosensors utilizing ZnO/MWCNTs nanocomposites have successfully demonstrated electroanalytic characters to detect glucose and ascorbic acid in simulated body fluid. The sensor design shows that MWCNTs are chemisorbed on the surface of ZnO through the -COOH group with nonhomogeneous surface coverage. Of the six variations of the MWCNTs mass fraction, the resulting current response of cyclic voltammetry to the ZnO electrode doped with 2% MWCNTs showed the highest sensitivity of glucose and ascorbic acid measurement which is most likely due to the greater total surface reactivity and the lower defect concentration compared to other nanocomposites. Furthermore, despite the linear behavior of impedance response, the currently developed system cannot distinguish the frequency response associated to glucose and ascorbic acid.

ACKNOWLEDGMENT

The author would like to thank for financial support from LPPM Institut Teknologi Sepuluh Nopember (ITS) for research grants "Penelitian Pemula" agreement No: 1373/PKS/IT / 2018.

REFERENCES

1. Akyazi T, Basabe-Desmonts L, Benito-Lopez F. Review on microfluidic paper-based analytical devices towards commercialisation. *Analytica chimica acta* 2017.
2. Martinez AW, Phillips ST, Nie Z, Cheng CM, Carrilho E, Wiley BJ, Whitesides GM. Programmable diagnostic devices made from paper and tape. *Lab on a Chip* 2010; 19:2499-2504.
3. Songjaroen T, Dungchai W, Chailapakul O, Henry CS, Laiwattanapaisal W. Blood separation on microfluidic paper-based analytical devices. *Lab on a Chip* 2010; 12:3392-3398.
4. Wu G, Zaman MH. Low-cost tools for diagnosing and monitoring HIV infection in low-resource settings. *Bulletin of the World Health Organization* 2012; 90:914-920.
5. Dungchai W, Chailapakul O, Henry CS. Electrochemical detection for paper-based microfluidics. *Analytical chemistry* 2009; 81:5821-5826.
6. Hu J, Wang S, Wang L, Li F, Pingguan-Murphy B, Lu TJ, Xu F. Advances in paper-based point-of-care diagnostics. *Biosensors and Bioelectronics* 2014; 54:585-597.
7. Li X, Ballerini DR, Shen W. A perspective on paper-based microfluidics: current status and future trends. *Biomicrofluidics*. 2012; 6:011301.
8. Jagadeesan KK, Kumar S, Sumana G. Application of conducting paper for selective detection of troponin. *Electrochemistry Communications* 2012; 20:71-74.
9. Yetisen AK, Akram MS, Lowe CR. Based microfluidic point-of-care diagnostic devices. *Lab on a Chip* 2013; 13:2210-2251.
10. Gabriel EF, Garcia PT, Cardoso TM, Lopes FM, Martins FT, Coltro WK. Highly sensitive colorimetric detection of glucose and uric acid in biological fluids using chitosan-modified paper microfluidic devices. *Analyst* 2016; 141:4749-4756.
11. Santhiago M, Henry CS, Kubota LT. Low cost, simple three dimensional electrochemical paper-based analytical device for determination of p-nitrophenol. *Electrochimica Acta* 2014; 130:771-777.
12. Wahyuono RA, Roekmono R, Hadi H, Yuwono RA, Muhimmah LC. Deteksi Kadar Glukosa Dalam Plasma Darah Terpisah Oleh Mikrofluida Terintegrasi Partikel Nano ZnO Berbasis Spektroskopi Inframerah Dan Raman. *Jurnal Integrasi Proses* 2017; 6, :148-154.
13. Yuwono RA, Izdiharruddin MF, Wahyuono RA. Integrated ZnO nanoparticles on paper-based microfluidic: toward efficient analytical device for glucose detection based on impedance and FTIR measurement. *Proc. SPIE 10150, Second International Seminar on Photonics, Optics, and Its Applications (ISPhOA 2016)*, 1015011 (11 November 2016); doi: 10.1117/12.2243827.
14. Li X, Zhao C, Liu X. A paper-based microfluidic biosensor integrating zinc oxide nanowires for electrochemical glucose detection. *Microsystems & Nanoengineering* 2015; 1:15014.
15. Muhimmah LC, Roekmono, Hadi H, Yuwono RA, Wahyuono RA. Blood plasma separation in ZnO nanoflowers-supported paper based microfluidic for glucose sensing. *AIP Conference Proceedings* 2018; 1945:020006.
16. Roekmono, Hadi H, Muhimmah LC, Imtihani HN, Yuwono RA, Wahyuono RA. Glucose and Cholesterol Sensing in Blood Plasma using ZnO-Paper Based Microfluidics. *International Journal of Drug Delivery and Technology* 2018, accepted.
17. Wahyuono RA, Risanti DD, Shirotsaki T, Nagaoka S, Takafuji M, Ihara H. Photoelectrochemical performance of DSSC with monodisperse and polydisperse ZnO SPs. *AIP Conference Proceedings* 2014; 1586:78-81.

18. Wahyuono RA, Schmidt C, Dellith A, Dellith J, Schulz M, Seyring M, Rettenmayr M, Plentz J, Dietzek B. ZnO nanoflowers-based photoanodes: aqueous chemical synthesis, microstructure and optical properties. *Open Chemistry* 2016; 14:158-169.
19. Wahyuono RA, Hermann-Westendorf F, Dellith A, Schmidt C, Dellith J, Plentz J, Schulz M, Presselt M, Seyring M, Rettenmeyer M. Effect of annealing on the sub-bandgap, defects and trapping states of ZnO nanostructures. *Chemical Physics* 2017; 483:112-121.
20. Syukron A, Wahyuono RA, Sawitri D, Risanti DD. The Effect of Paste Preparation and Annealing Temperature of ZnO Photoelectrode to Dye-Sensitized Solar Cells (DSSC) Performance. *Adv. Mater. Res* 2014; 896:183-186.
21. Kokubo T, Takadama H. How useful is SBF in predicting in vivo bone bioactivity? *Biomaterials* 2006; 27:2907-2915.
22. Pandey P, Parra MR, Haque FZ, Kurchania R. Effects of annealing temperature optimization on the efficiency of ZnO nanoparticles photoanode based dye sensitized solar cells. *Journal of Materials Science: Materials in Electronics* 2017; 28:1537-1545.
23. Dobrzańska-Danikiewicz A, Łukowiec D, Cichocki D, Wolany W. Carbon nanotubes manufacturing using the CVD equipment against the background of other methods. *Archives of Materials Science and Engineering* 2013; 64:103-109.
24. Wisitsoraat A, Karuwan C, Wong-ek K, Phokharatkul D, Sritongkham P, Tuantranont A. High sensitivity electrochemical cholesterol sensor utilizing a vertically aligned carbon nanotube electrode with electropolymerized enzyme immobilization. *Sensors* 2009; 9:8658-8668.
25. Chen R, Li Y, Huo K, Chu PK. Microelectrode arrays based on carbon nanomaterials: emerging electrochemical sensors for biological and environmental applications. *RSC Advances* 2013; 3:18698-18715.
26. Rusu MM, Wahyuono RA, Fort CI, Dellith A, Dellith J, Ignaszak A, Vulpoi A, Danciu V, Dietzek B, Baia L. Impact of drying procedure on the morphology and structure of TiO₂ xerogels and the performance of dye sensitized solar cells. *J. Sol-Gel Sci. Technol* 2017; 81:693-703.